

## Drug Delivery

## A Selective Release System Based on Dual-Drug-Loaded Mesoporous Silica for Nanoparticle-Assisted Combination Therapy

Wenqian Wang, Yongqiang Wen,\* Liping Xu, Hongwu Du, Yabin Zhou, and Xueji Zhang\*[a]

**Abstract:** A selective release system was demonstrated with a dual-cargo loaded MSNs. When stimulated by different signals (UV or H<sup>+</sup>), this system could selectively release different kinds of cargoes individually. Furthermore, this system has been used to provide a combination of chemotherapy

and biotherapy for cancer treatment. This controlled release system could be an important step in the development of more effective and sophisticated nanomedicine and nanodevices, due to the possibility of selective release of a complex multi-drug.

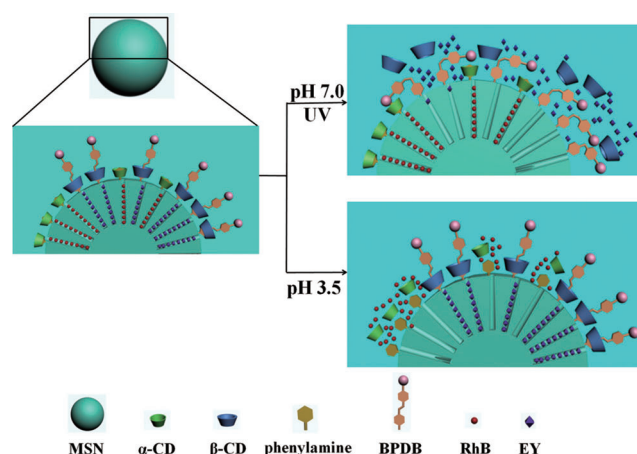
## Introduction

The controlled release system, which has been widely used in drugs delivery, cell imaging, disease diagnosis, catalysis, and environmental protection, has gained much attention in the past couple of decades.<sup>[1–4]</sup> In particular, it shows important applications in the treatment of severe diseases. Cancer is one of the most serious diseases that threaten human beings today. So far, multiple cancer treatment technologies, such as surgical resection, radiotherapy, chemotherapy, thermotherapy, biotherapy, and gene therapy, have been widely used to treat cancer; however, they all have their own limitations. For example, chemotherapy, as the most common method for cancer treatment, has the problem of cancer chemoresistance, which leads to most of the failed cases in cancer therapy.<sup>[5]</sup> These challenges have driven researchers and clinicians to investigate clever and elegant approaches to overcome these limitations. The combination of multiple therapy technologies/drugs has been regarded as one of the most promising treatment strategies, which can reduce the side effects, suppress drug resistance, and strengthen the antitumor effect through distinct mechanisms of action.<sup>[5,6]</sup>

As one of the most extensively studied controlled-release platforms, the mesoporous silica nanoparticle (MSN) is especially attractive for its large surface exteriors, porous interiors, biocompatibility and the ability to chemically modify its surface.<sup>[7]</sup> To date, many delicate intelligent switches had been implemented by other researchers and ourselves to trigger the opening of the pores and the release of encapsulated car-

goes.<sup>[8]</sup> In spite of the substantial progress, most of these controlled-release systems contain only one kind of cargo. Recently, some controlled-release systems loaded with multiple cargoes had been designed. However, these systems were limited to release the multiple cargoes simultaneously or release them in sequence in different size ranges.<sup>[9]</sup> It still remains a grand challenge to develop a multi-cargo-loaded system that can control the release of each cargo independently at will.

In this paper, a selectively controlled-release system was demonstrated through a dual-cargo-loaded MSNs system (Scheme 1). In this system, the supramolecular pseudorotaxanes were used to trap two kinds of cargoes into the nanopores of MSNs individually. These nanopores were radially oriented and unconnected between each other. Under the stimuli of different signals, UV or H<sup>+</sup>, the dual cargoes could be selectively released from the MSNs separately. In the neutral solution, only one cargo could be released from the MSNs under the irradiation of UV; and whether UV or not, only another



**Scheme 1.** The release process of the dual-dye-loaded MSNs. The dual dyes were loaded into the MSNs separately by pH-controlled nanogates and UV-controlled nanovalves. This system can selectively release Eosin Yellowish (EY) upon UV irradiation (at pH 7.0) and Rhodamine B (RhB) at pH 3.5.

[a] Dr. W. Wang, Prof. Y. Wen, Prof. L. Xu, Prof. H. Du, Y. Zhou, Prof. X. Zhang  
Research Center for Bioengineering &  
Sensing Technology, School of Chemistry &  
Biological Engineering, University of Science and  
Technology Beijing, Beijing 100083 (P.R. China)  
E-mail: wyq\_wen@iccas.ac.cn  
zhangxueji@ustb.edu.cn

Supporting information for this article is available on the WWW under  
<http://dx.doi.org/10.1002/chem.201402334>.

cargo could be released from the MSNs upon the stimulus of  $H^+$ . In consideration of the low pH of intracellular lysosome and nearly neutral pH of most extracellular fluids, the selective release system had been further applied to release two kinds of antitumor agents in the intracellular and extracellular environment of tumor cell, individually, which take effect on tumor cells through chemotherapy and biotherapy, respectively. Under the combination of two cancer treatment technologies, the inhibitory rate of tumor cells A549 was evidently increased with respect to a single treatment. This research has made an important progress in MSNs-based intelligent controlled-release system. The selective controlled-release system would allow more accurate and controllable release for a sophisticated drug delivery, and could have the potential to treat human diseases effectively with combination therapies and diagnosis.

## Results and Discussion

As shown in Figure 1, MSNs were obtained by using the modified base-catalyzed sol-gel method with an average diameter of 350 nm.<sup>[10]</sup> The mesoporous channel could be clearly observed by transmission electron microscopy.  $N_2$  sorption analysis of the MSN exhibited a type IV isotherm with a total surface area (Brunauer-Emmett-Teller, BET) of  $1766.59 \text{ m}^2 \text{ g}^{-1}$  and an average pore diameter of 4.4 nm. The nanoparticles also showed typical XRD patterns of MCM-41 type hexagonal mesoporous silica with a lattice spacing of about 4.3 nm.

(*E*)-4-((4-(Benzylcarbamoyl)phenyl)diazenyl) benzoic acid (BPDB) was firstly synthesized by the dehydration between azobenzene-4, 4'-dicarboxylic acid and benzylamine (Figure S1, the Supporting Information).<sup>[11a]</sup> MSNs were treated with 3-aminopropyltriethoxysilane (APTES) to get the amine-modified MSNs (MS- $NH_2$ ). Then, the MS- $NH_2$  was modified with BPDB and N-phenylaminopropyltrimethoxysilane (PhAPTMS) step by step to afford the phenylamine group (Ph) and BPDB dual-

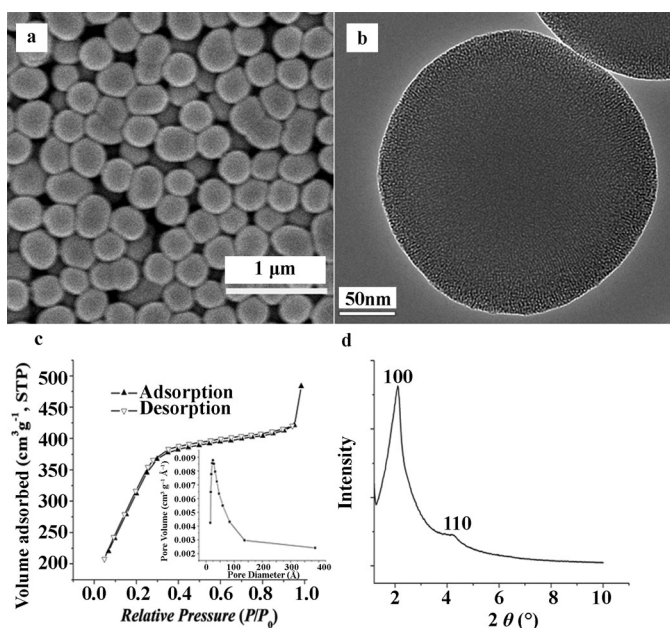
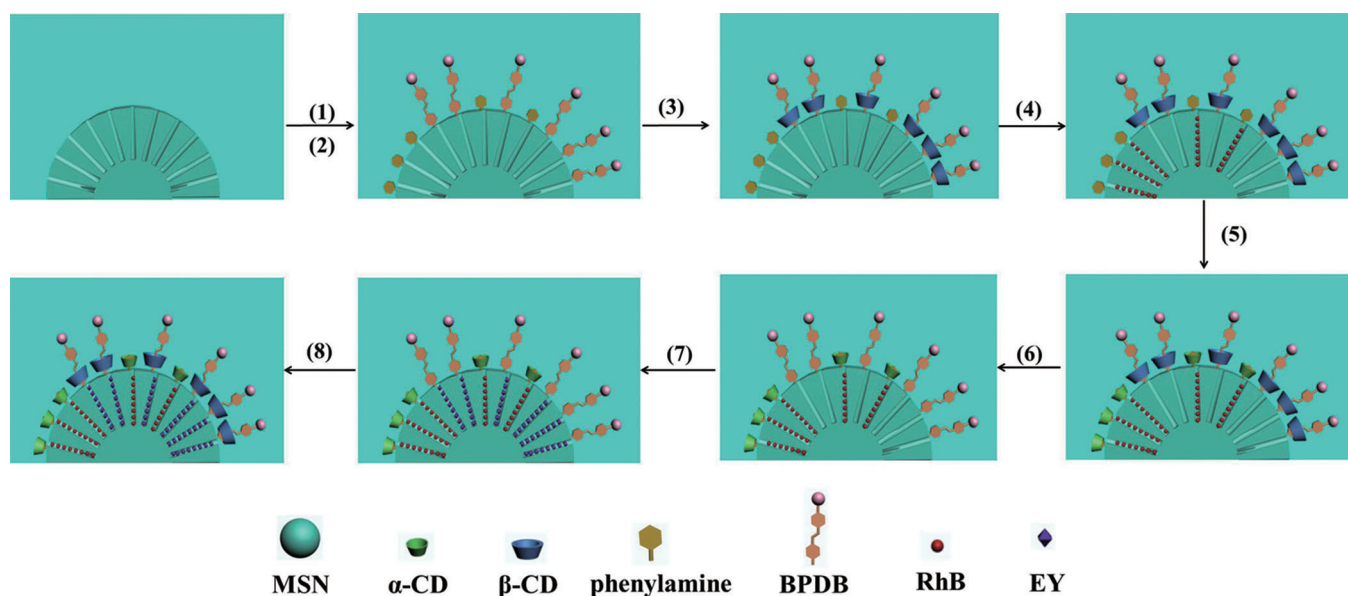


**Figure 1.** a) SEM: The average diameter of MSN was 350 nm. b) TEM: The mesoporous channels were clearly observed. The scale bar corresponds to 50 nm. c)  $N_2$  sorption isotherm. Inset: pore size distribution. d) XRD.

functional MSNs (MS-PhBPDB; Scheme 2 and Figure S2, the Supporting Information). In the UV/Vis spectrum of MS-PhBPDB (Figure 2), the absorption peak at 250 nm was attributed to the benzene group, and the absorption peak at 340 nm was produced by azobenzene group.

As has been frequently reported in literature,<sup>[11]</sup>  $\alpha$ -cyclodextrins ( $\alpha$ -CD) have a strong propensity for binding with the Ph group and a much weaker propensity with protonated Ph group. And because of the much lower efficient photoisomerization of azobenzene unit in acidic solution,<sup>[12]</sup>  $\beta$ -cyclodextrins



**Scheme 2.** Preparation of the dual-dye loaded MSNs. (1) APTES, BPDB; (2) PhAPTMS; (3)  $\beta$ -CD; (4) RhB; (5)  $\alpha$ -CD; (6) UV light; (7) EY; (8)  $\beta$ -CD.

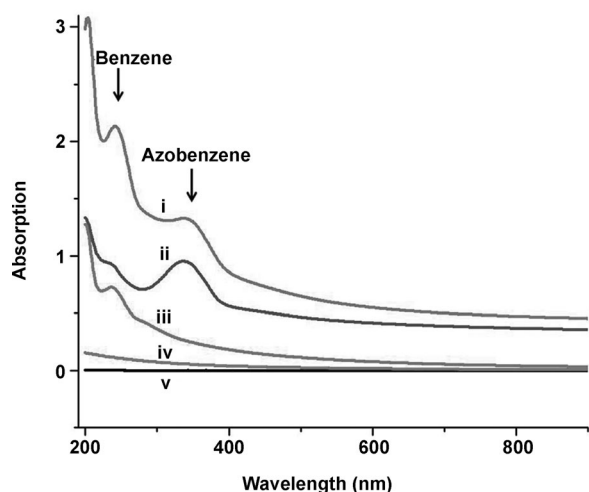


**Figure 2.** The UV/Vis absorption spectra of the aqueous solution of different functional MSNs ( $1 \text{ mg mL}^{-1}$  MSNs; i: MS-PhBPDB; ii: MS-BPDB; iii: MS-Ph; iv: MS; v: control). The absorption peak at 250 nm was attributed to the benzene group, and the absorption peak at 340 nm was produced by the azobenzene group.

( $\beta$ -CD) can only reversibly bind with azobenzene unit through the *trans*-*cis* photoisomerization of azobenzene unit under UV irradiation in neutral conditions (Figure S4, the Supporting Information). Therefore, a supramolecular pseudorotaxanes system containing the  $\alpha$ -CD rings on PhAPTMS grafting a Ph group can act as "gatekeepers" of the nanopores on the MSNs. This system blocks the departure of cargo molecules at physiological conditions, as well as another pseudorotaxanes assembled by  $\beta$ -CD rings threading onto BPDB stalks containing an azobenzene group. These two supramolecular structures, Ph/ $\alpha$ -CD and BPDB/ $\beta$ -CD, could be disassociated to unblock the nanopores of MSNs by decreasing the pH value of external medium and UV irradiation at pH 7.0, individually. In addition, the binding affinity between  $\alpha$ -CD and azobenzene group or between  $\beta$ -CD and the Ph group is much lower to assemble the stiff pseudorotaxanes structures for capping the nanopores on the MSNs (Figure S5 and S6, the Supporting Information). For above all, the method of "close one, open another" was employed to load Rhodamine B (RhB) with Ph/ $\alpha$ -CD nanovalves and Eosin Yellowish (EY) with BPDB/ $\beta$ -CD nanovalves into the MS-PhBPDB, respectively (Scheme 2). In a typical experiment, the pores modified by BPDB were firstly capped by  $\beta$ -CD to stop the cargoes diffusing into these pores. With one kind of the fluorescent molecules (RhB) loaded into the open nanopores, these nanopores were locked by  $\alpha$ -CD rings binding to Ph-containing stalks. Subsequently, the RhB-loaded MSNs were irradiated by UV light to disassociate the  $\beta$ -CD rings from the BPDB stalks and open the nanopores that were capped by  $\beta$ -CD. Then, the other kind of fluorescent molecules, EY, were trapped into these pores by  $\beta$ -CD rings threading onto the BPDB stalks. Fluorescence intensity at 540 (EY) and 575 nm (RhB) was used to monitor the signals of released cargo molecules from the dual-dye loaded MSNs.

As illustrated in Figure 3, when the dual-dye loaded MSNs were tested without a cyclodextrin cap, the dyes could not be

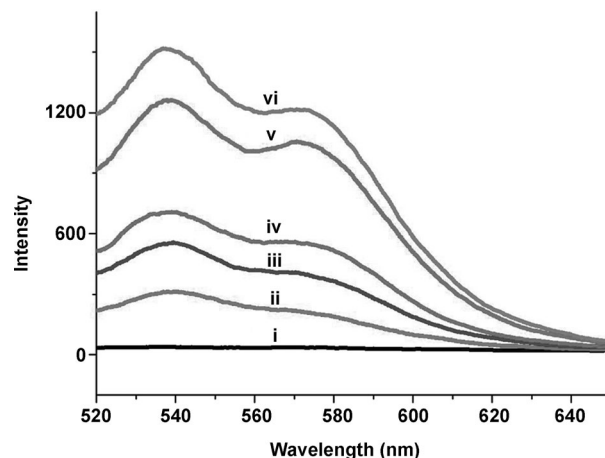


**Figure 3.** Release behavior of dual-cargo-loaded MS-PhBPDB, without capped cyclodextrins, at pH 7.0 without UV irradiation. This demonstrates that the dual cargoes could be released from the MS-PhBPDB simultaneously without the CD capped in the aqueous solution (i: 0; ii: 0.5; iii: 1.0; iv: 1.5; v: 3.0; vi: 4.0 h).

prevented from leaking from the MSNs at pH 7.0, and the two kinds of dyes escaped from the nanopores simultaneously. However, in the presence of cyclodextrins, none of the two dyes were observed at the conditions of pH 7.0 without the irradiation of UV. The flat baseline indicates that both of the two dyes were not released in the neutral solution (Figure 4a and 4b). The results proved that the complexes of Ph/ $\alpha$ -CD and BPDB/ $\beta$ -CD had formed the stiff structure of pseudorotaxanes to cap the pores of the MSNs in neutral solution. Hence, both of the dyes could not be released from the nanopores.

The dual-dye-loaded MSNs were then irradiated by UV light, while the external medium was maintained at pH 7.0. The result showed that a rapid increase in the emission intensity

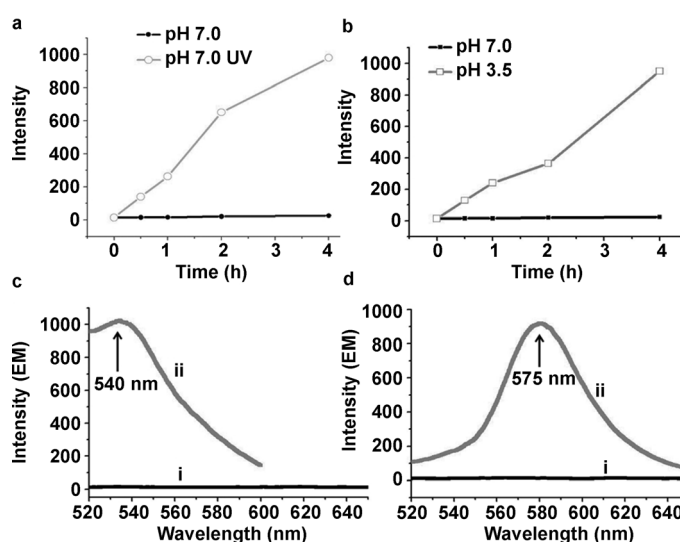


**Figure 4.** The release behavior of dual-dye-loaded MSNs controlled by single stimulus. a) UV-light dependence of the release profiles of EY and b) pH dependence of the release profiles of RhB from the MSNs system. c, d) Fluorescence spectra of dual-dye loaded MSNs before (i) and after (ii) irradiating with UV light at pH 7.0 or lowering the pH to 3.5 for 4 h.

around 540 nm occurred, whereas another emission signal (575 nm) was not observed at all. The results indicated that the EY was released from the nanopores of the MSNs, but RhB was still retained in the MSNs upon UV-light irradiation. This consequence could be attributed to the conformational changes of the azobenzene unit of BPDB from the more stable *trans* to the less stable *cis* configuration. The isomerization of the azobenzene unit led to the dissociation of pseudorotaxanes (BPDB/ $\beta$ -CD). The  $\beta$ -CD rings were unthreaded from the BPDB stalks and they unblocked the nanopores sealed by the BPDB/ $\beta$ -CD complex. Under the same conditions, the pseudorotaxanes of Ph/ $\alpha$ -CD were still stable and stopped the RhB escaping from the MSNs. Therefore, only EY molecules were released from the nanopores of MSNs (Figure 4a and c).

When the pH value of the solution was adjusted to 3.5 and no UV light was provided, an obvious increase in the emission intensity only around 575 nm occurred, indicating that the RhB escaped from the nanopores of the MSNs upon lowering the pH, whereas the EY was still sustained in the MSNs. The addition of H<sup>+</sup> could lead to the protonation of Ph group, and the binding affinity between  $\alpha$ -CD and the Ph group would be diminished, causing the dissociation of the  $\alpha$ -CD rings from the PhAPTMS stalks. The  $\alpha$ -CD rings unblocked the nanopores modified by the PhAPTMS and allowed the RhB to escape into solution. Under the same conditions, the  $\beta$ -CD rings did not unthread from azobenzene-containing BPDB stalks in the acid solution (Figure 4b and 4d). The fluorescence spectra of the release system (Figure 4c and 4d) after UV irradiation and H<sup>+</sup> addition showed dramatically different characteristic peaks, which proved that the dual-dye-loaded MSNs can selectively release the EY or RhB molecules in response to different external stimuli.

When the pH of the solution was adjusted to 3.5, the MSNs were simultaneously irradiated by UV light. Interestingly, the dual dyes, EY and RhB, did not release from the nanopores at the same time. As shown in the fluorescence spectra, we can only find the signal of RhB in the solution (Figure 5). In other words, whether irradiating UV light or not, the nanopores modified by BPDB stalks would be capped by pseudorotaxanes of BPDB/ $\beta$ -CD constantly in acid solution. This consequence may be attributed to the presence of the nitrogen atoms on the BPDB stalks.<sup>[12]</sup> In acid solution, the protonation of the benzylamine and two nitrogen atoms of the azobenzene group re-

duced the rate of photoisomerization to inhibit the  $\beta$ -CD rings unthreaded from the BPDB stalks under UV irradiation. Therefore, EY was still stored in the nanopores of MSNs and no release of EY was observed under these conditions.

As a preliminary application research, the tests of cell viability were further carried out to evaluate the combination therapy efficiency of the selective release system on A549 cell lines. By using a combination of chemotherapy and biotherapy, different kinds of antitumor agents could take effect at individual active sites, at specific times and in a different dosage. The bio-antitumor agents can bind the receptor on the surface of the tumor cell to induce tumor cell apoptosis in extracellular environment, whereas most of the chemotherapy drugs take effect in an intracellular environment.<sup>[13]</sup> In our experiment, octreotide acetate (OCT) and epirubicin (EPB) were used as the model biotherapy and chemotherapy antitumor agents to load into the MS-PhBPDB step by step. OCT, a kind of somatostatin analogue, has antitumor activities mediated through somatostatin receptors over-expressed on the surface of tumor cells in extracellular environment; whereas EPB could embed into two nucleic acid bases to kill the tumor cells through interfering the transcription process and inhibiting the synthesis of DNA and RNA after entering the tumor cells. For the reason of the low pH of intracellular lysosome and nearly neutral pH of most extracellular fluids, the UV-responsive nanogates on the MS-PhBPDB could control the drugs to release under the stimulus of UV irradiation only in extracellular environment but not in an intracellular environment; and, the pH-responsive nanogates could control the drugs to release only in intracellular environment after the MS-PhBPDB entered into the cell through endocytosis.

In our experiment, EPB and OCT were loaded into the MS-PhBPDB by pH-controlled and UV-controlled nanovalves, respectively. A549 cells were incubated with this dual-drug-loaded MS-PhBPDB for 4 h, and then washed twice with PBS buffer before adding fresh growth medium for further incubation 24 h. As shown in Figure 6a ii, the viability of the A549 cells decreased to 42.83% compared with the control (Figure 6a i). Considering that the lower pH of tumor interior tissues, endosomes and lysosomes, the result could be attributed to the release of EPB from MS-PhBPDB, which entered into the tumor cells through endocytosis. In addition, the mixture of cell cultures and MS-PhBPDB was irradiated by UV for 15 min and incubated in dark. After 24 h, the cell cultures were separated from the MS-PhBPDB and incubated with the tumor cells for another 24 h. As shown in Figure 6a iii, the viability of A549 cells decreased to 57.07% due to the apoptosis of tumor cells induced by the release of OCT. Finally, the dual-drug-loaded MS-PhBPDB was incubated with A549 cells and irradiated immediately with UV for 15 min. The viability of the cells decreased significantly to 26.55% after 24 h (Figure 6a iv, Figure 6b), which could be attributed to the combination therapy of OCT and EPB at the extracellular and intracellular environment. In this case, the UV-controlled nanogates were firstly opened to release OCT before the particles entering into the cells. Then, EPB was sequentially released from the MS-PhBPDB

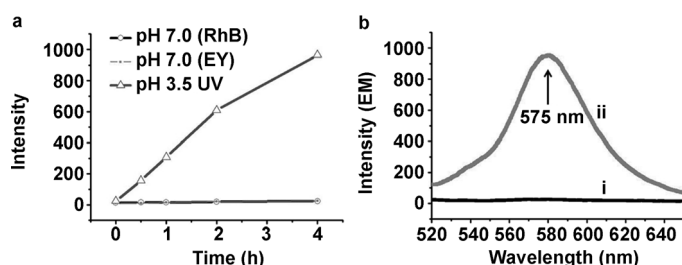


**Figure 5.** The release behavior of dual-dye-loaded MSNs controlled by dual stimuli. a) The release profiles of the MSNs upon UV irradiation at pH 3.5. b) Fluorescence spectra of dual-dye-loaded MSNs before (i) and after (ii) irradiating with UV light in pH 3.5 for 4 h.

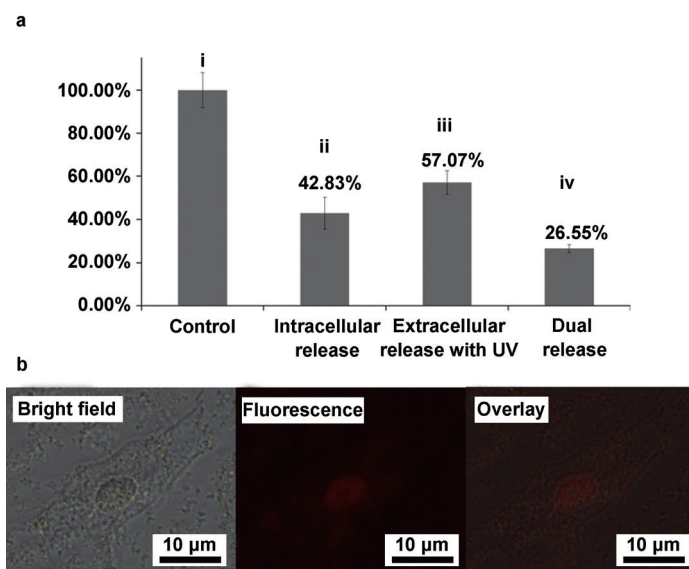


**Figure 6.** a) Viability test of A549 cells with dual-drug-loaded MS-PhBPDB ( $50 \mu\text{g mL}^{-1}$ ) after 24 h incubation, in which was loaded EPB and OCT by pH-controlled nanogates and UV-controlled nanovalves, respectively ( $P < 0.01$ ). b) The images of A549 cells under the combination therapy of OCT and EPB. The scale bar corresponds to  $10 \mu\text{m}$ .

system after the MS-PhBPDB had been taken-up into the A549 cells.

In a contrast experiment, OCT and EPB were loaded into the MS-PhBPDB by pH-controlled and UV-controlled nanovalves, respectively. After the MS-PhBPDB entered into the cells, the viability of A549 did not obviously decrease for the OCT releasing at the intracellular environment, indicating that was an improper delivery site for OCT (A549 = 92.07%, Figure S11 ii and S13 A, the Supporting Information). Meanwhile, EPB was not released after the MS-PhBPDB entered into the A549 under UV irradiation; it can only be released when the MS-PhBPDB is located at the neutral environment (Figure S11 iii, iv, and Figure S12 B, the Supporting Information).

The cell experiments indicated that the UV-responsive nanogates could control the release of bio-antitumor agent, which only takes effect in the extracellular environment of the tumor; whereas the pH-responsive nanogates could control the chemotherapy drugs to be released only in intracellular environment of the tumor. These results further proved that a high antitumor efficiency could only be realized when specific antitumor agents were delivered and released, and only played an active role at specific situations. Therefore, a precise, controllable, multidrug delivery system was pivotal for enhancing antitumor efficiency and reducing the side effects.

## Conclusion

We report here an intelligent MSNs-based multidrug selective release system. This system could selectively release different cargoes under the stimuli of different signals. This system was further applied to the combination of chemotherapy and biotherapy of cancer through loading and releasing two kinds of antitumor agents at intracellular and extracellular environment of the tumor cell, respectively. The selectively controlled re-

lease allowed more accurate and controllable drug delivery and high efficient therapy. The approaches of selectively controlled release and combined therapy could be expected to be further extended to more practical system, for example, the release system activated by near-infrared (NIR), cancer biomarkers, and so on, and it could also be applied to the multiple combination therapy with other treatment methods.

## Experimental Section

### Materials

Tetraethoxysilane (TEOS, 99.9%), *n*-cetyltrimethylammonium bromide (CTAB,  $\geq 99\%$ ), 3-aminopropyltriethoxysilane (APTES, 99%), *N*-phenylaminopropyltrimethoxysilane (PhAPTMS), Rhodamine B, Eosin Yellowish, azobenzene-4, 4'-dicarboxylic acid and 3-[4,5-dimethylthiazol-2-yl]-2,5-diphenyltetrazolium bromide (MTT,  $\geq 98\%$ ) were purchased from Sigma Company. Benzylamine, thionyl chloride, pyridine, sodium hydroxide, disodium hydrogen phosphate dodecahydrate, dimethyl sulfoxide, and citric acid were purchased from Sinopharm Chemical Reagent Co. Ltd. Octreotide acetate (OCT) and epirubicin (EPB) were purchased from Chengdu Kaijie Biopharm Co. Ltd. and Pfizer. RPMI Medium 1640 and fetal bovine serum (FBS) were purchased from life technologies. All buffers were prepared with ultra-pure MilliQ water (resistance  $> 18 \text{ M}\Omega \text{ cm}^{-1}$ ).

### Instruments

Scanning electron microscopy (SEM) was performed with a JEOL-6700FE instrument. Transmission electron microscopy (TEM) images were obtained by using a TecnaiG2 F20 electron microscope. Powder X-ray diffraction (XRD) patterns were collected using a Rigaku D/max 2500 equipped with  $\text{Cu}_{\text{K}\alpha}$  radiation. UV/Vis spectra were collected using a Shimadzu U-1800 spectrophotometer. All fluorescence spectra were recorded on a Hitachi F-4500 FL Spectrophotometer in PBS buffer. Thermal stability measurements were collected on DTG-60 (Shimadzu Instruments) between 100 and  $550^\circ\text{C}$  with a heating rate of  $10^\circ\text{C min}^{-1}$ .  $\text{N}_2$  adsorption-desorption isotherms were obtained at 77 K on a Micromeritics ASAP2020 automated sorption analyzer. The BET model was applied to evaluate the specific surface areas. Pore size and pore volume were determined from the adsorption data by the BJH method.  $^1\text{H}$  NMR spectra (400 MHz) were recorded on a Bruker DPX 400 MHz spectrometer in  $\text{CDCl}_3$ .

### Syntheses

**BPDB:** Azobenzene-4, 4'-dicarboxylic acid (0.20 g, 0.74 mmol) was stirred with thionyl chloride (0.19 g, 1.6 mmol) and pyridine (0.16 g, 2.0 mmol) in  $\text{CH}_2\text{Cl}_2$  for 1 h followed by addition of benzylamine (0.08 g, 0.74 mmol). The mixture was stirred at room temperature until complete disappearance of starting material as verified by TLC ( $\approx 2\text{--}3$  h). After removal of the solvent, the residue was purified by column chromatography ( $\text{CHCl}_3/\text{MeOH}$  10:1) to afford pure BPDB as a yellow oil (0.20 g, 74%).  $^1\text{H}$  NMR (400 MHz,  $\text{CDCl}_3$ ,  $25^\circ\text{C}$ , TMS):  $\delta = 3.96$  (s, 2H,  $\text{CH}_2$ ), 7.40–7.26 (m, 6H), 7.99–7.97 (t, 6H), 8.20 (d, 1H), 8.22 ppm (d, 1H);

**MSN:** *N*-Cetyltrimethylammonium bromide (CTAB, 0.5 g) was mixed with water (42 mL), ethanol (18 mL) and solution of sodium hydroxide (0.6 mL, 2 mol L<sup>-1</sup>) under stirring for 30 min. Then, tetraethoxysilane (TEOS, 2.8 mL) was once added to the mixture, which was stirred at room temperature for 8 h. The resulting MSNs were separated by centrifugation, washed several times with water and ethanol, and dried in the oven (60 °C) overnight. Removal of template was achieved by solvent extraction: MSNs (1.0 g) were suspended in ethanol (100 mL) and 37% HCl (2 mL), and the mixture was heated under reflux for 24 h. The solvent-extracted particles were washed extensively with ethanol and collected through centrifugation.

**MS-PhBPDB:** BPDB and phenylamine group-functionalization of the silica surface was performed by suspending the MSNs (100 mg) in a solution of 3-aminopropyltriethoxysilane (11 μL, 0.05 mmol) in dry toluene (10 mL) for 30 min. The toluene was then removed by centrifugation. The nanoparticles were washed with toluene, ethanol, and dried under vacuum, to give MS-NH<sub>2</sub> (89.10 mg, 77.23%). BPDB (17.97 mg, 0.05 mmol) was dissolved in dried toluene (5 mL). The solution was added to flask containing 3-aminopropyltriethoxysilane-coated MSNs (50 mg). The solution was mixed and sonicated to disperse nanoparticles. The solution was then allowed to stir under room temperature for 24 h, to give MS-BPDB (43.43 mg, 68.00%). MS-BPDB (50 mg) was treated with PhAPTMS (6 μL, 0.025 mmol) in dried toluene (10 mL) and allowed to heat at reflux under N<sub>2</sub> for 24 h, to give MS-PhBPDB (47.01 mg, 62.41%). The nanoparticles were separated from solution by centrifugation and washed with toluene and ethanol, in turn. The particles were dried under vacuum overnight.

**Dual dyes loaded in the MS-PhBPDB:** Firstly, β-CD (56.75 mg, 0.05 mmol) was added to an aqueous solution containing MS-PhBPDB (50 mg) to cap the nanopores near the BPDB stalks on the surface of nanoparticles. Then, the pH-controlled nanopores were opened by dispersing the MSNs in acid solution (pH 3.5) and recovered by washing the nanoparticles with a neutral buffer solution. Secondly, the loading of RhB into MSNs was achieved by soaking MS-PhBPDB (50 mg) in the an aqueous solution (10 mL) containing RhB (0.8 mL, 0.1 mmol L<sup>-1</sup>) for about 24 h. Subsequently, α-CD (48.64 mg, 0.05 mmol) was added to the solution and incubated overnight to cap the nanopores controlled by pH. Next, the RhB-loaded MSNs were irradiated by UV for 24 h to open the nanopores beside the azobenzene unit-containing stalks (washed the MSNs in each 4 h). Finally, we used the way of loading RhB to load the EY (0.4 mL, 0.1 mmol L<sup>-1</sup>) into the nanopores controlled by UV and capped by β-CD again to obtain the dual-dye-loaded MS-PhBPDB (49.2 mg, 59.58%).

**Testing the dye release:** The release signal was investigated by monitoring the fluorescence intensity of the release system. Dual-dye-loaded MSNs (3 mg) were placed in a bottom corner of cuvette, and the PBS solution (citric acid/disodium hydrogen phosphate) was then carefully filled to avoid disturbing the MSNs. Under some stimuli, the dyes would be released into the solution. Without stimuli, the dyes would not be released from the MSNs and diffused into the solution. Then, the solution could be directly monitored by fluorescence spectrophotometer to record the release of dyes. For activating the nanomachines, the pH of the solution was decreased or MSNs were irradiated with UV-light, respectively. The amount of released guest molecules from the pores of MSNs was monitored by the change of the fluorescent intensity at 540 and 575 nm.

## The studies of inhibition rate of A549 cells with OCT and EPB

The A549 cells were placed on 96 wells cell culture clusters at a density of 1 × 10<sup>4</sup> cells per well and cultured in 5% CO<sub>2</sub> at 37 °C for 12 h. Then, a different density of OCT and EPB were added to the media, respectively, and the A549 cells were incubated in 5% CO<sub>2</sub> at 37 °C for 24 h. Cell viability was determined by the standard MTT assay.

## The biocompatibility studies of MS-PhBPDB and UV light

A549 cells were plated on 96 wells cell culture clusters at a density of 1 × 10<sup>4</sup> cells per well and cultured in 5% CO<sub>2</sub> at 37 °C for 12 h. Then, MS-PhBPDB (100 μL, 50 μg mL<sup>-1</sup>) were added to the media and irradiated by UV for 15 min, and the cells were incubated in 5% CO<sub>2</sub> at 37 °C for 24 h. Cell viability was determined by the standard MTT assay.

## Cell experiment

To test the release of the drugs in the cell line, A549 cells were placed on 96 well cell culture clusters at a density of 1 × 10<sup>4</sup> cells per well and cultured in 5% CO<sub>2</sub> at 37 °C for 12 h. Before the loading of the OCT and EPB, a solution of OCT (50 mg L<sup>-1</sup>) and EPB (125 μmol L<sup>-1</sup>) had been prepared. Then, the MS-PhBPDB was divided into two groups, and these two antitumor agents were loaded in the same way as the loading of the dyes. Group I contained trapped OCT with Ph/α-CD nanovalves and EPB with BPDB/β-CD nanovalves into the MS-PhBPDB, respectively. Group II contained trapped OCT with BPDB/β-CD nanovalves and EPB with Ph/α-CD nanovalves into MS-PhBPDB, respectively. Subsequently, assisted with ultrasonication, the two groups of dual-drug-loaded MS-PhBPDB were dispersed in cell culture fluid (100 μL, 50 g mL<sup>-1</sup>, 1640 medium + 8% FBS), and added to the media, separately. Next, the two groups were irradiated by UV for 15 min and incubated in 5% CO<sub>2</sub> at 37 °C without visual light. After 24 h, cell viability was determined by the standard MTT assay.

## Test for the extracellular and intracellular release of dual-drug-loaded MS-PhBPDB

A549 cells were placed on 96 well cell culture clusters at a density of 1 × 10<sup>4</sup> cells per well and cultured in 5% CO<sub>2</sub> at 37 °C for 12 h. The two groups MS-PhBPDB (100 μL, 50 μg mL<sup>-1</sup>) was added to the media, then A549 cells were incubated with dual-drug-loaded MS-PhBPDB for 4 h, and then washed with PBS twice before adding fresh growth medium for further incubation 24 h. As a control experiment, the two groups were irradiated by UV for 15 min after adding fresh growth medium. Cell viability was determined by the standard MTT assay. In addition, the two groups MS-PhBPDB (50 μg mL<sup>-1</sup>) were also placed at the corner of the quartz cuvette, then the cell culture fluid was added into the cuvette. After 24 h, the cell culture fluid was incubated with cells for another 24 h. As a control experiment, the mixture of cell culture fluid and dual-drug-loaded MS-PhBPDB were irradiated with UV for 15 min and placed in dark for 24 h. Then, the cell culture fluid was incubated with cells for another 24 h. Cell viability was determined by the standard MTT assay.

## Acknowledgements

The authors would like to thank the NSFC (21171019, 21073203, 51373023, 21275017, 21127007, 21103009), Beijing Natural Science Foundation (2122038), and the Fundamental Research Funds for the Central Universities and NCET-11-0584.

**Keywords:** combination therapy · drug delivery · mesoporous materials · nanotechnology · selective release

- [1] a) I. I. Slowing, J. L. Vivero-Escoto, C. W. Wu, V. S.-Y. Lin, *Adv. Drug Delivery Rev.* **2008**, *60*, 1278–1288; b) C. R. Thomas, D. P. Ferris, J. H. Lee, E. Choi, M. H. Cho, E. S. Kim, J. F. Stoddart, J. S. Shin, J. Cheon, J. I. Zink, *J. Am. Chem. Soc.* **2010**, *132*, 10623–10625; c) J. N. Liu, W. B. Bu, L. M. Pan, J. L. Shi, *Angew. Chem.* **2013**, *125*, 4471–4475; *Angew. Chem. Int. Ed.* **2013**, *52*, 4375–4379.
- [2] R. C. Qian, L. Ding, H. X. Ju, *J. Am. Chem. Soc.* **2013**, *135*, 13282–13285.
- [3] a) P. K. Vemula, J. Li, G. John, *J. Am. Chem. Soc.* **2006**, *128*, 8932–8938; b) C. H. Lu, X. J. Qi, R. Orbach, H. H. Yang, I. Mironi-Harpaz, D. Seliktar, I. Willner, *Nano Lett.* **2013**, *13*, 1298–1302.
- [4] J. Y. Liu, D. A. Sonshine, S. Shervani, R. H. Hurt, *ACS Nano* **2010**, *4*, 6903–6913.
- [5] a) G. F. S. Dhara, V. Fendrich, D. Bedja, R. Beaty, M. Mullendore, C. Karikari, H. Alvarez, C. Iacobuzio-Donahue, A. Jimeno, K. L. Gabrielson, W. Matsui, A. Maitra, *Cancer Res.* **2007**, *67*, 2187–2196; b) B. Al-Lazikani, U. Banerji, P. Workman, *Nat. Biotechnol.* **2012**, *30*, 679–692; c) H. Thomas, H. M. Coley, *Cancer Control* **2003**, *10*, 159–165; d) N. R. Patel, B. S. Pattni, A. H. Abouzeid, V. P. Torchilin, *Adv. Drug Delivery Rev.* **2013**, *65*, 1748–1762.
- [6] a) G. Weckbecker, I. Lewis, R. Albert, H. A. Schmid, D. Hoyer, C. Bruns, *Nat. Rev. Drug Discovery* **2003**, *2*, 999–1017; b) J. J. Parry, M. Eiblmaier, R. Andrews, L. A. Meyer, R. Higashikubo, C. J. Anderson, B. E. Rogers, *Mol. Imaging* **2007**, *6*, 56–67.
- [7] a) E. Climent, R. Martinez-Manez, F. Sancenon, M. D. Marcos, J. Soto, A. Maquieira, P. Amoros, *Angew. Chem.* **2010**, *122*, 7439–7441; *Angew. Chem. Int. Ed.* **2010**, *49*, 7281–7283; b) D. C. Niu, Z. Ma, Y. S. Li, J. L. Shi, *J. Am. Chem. Soc.* **2010**, *132*, 15144–15147.
- [8] a) N. C. Fan, F. Y. Cheng, J. A. Ho, C. S. Yeh, *Angew. Chem.* **2012**, *124*, 8936–8940; *Angew. Chem. Int. Ed.* **2012**, *51*, 8806–8810; b) H. Y. Wen, C. Y. Dong, H. Q. Dong, A. J. Shen, W. J. Xia, X. J. Cai, Y. Y. Song, X. Q. Li, Y. Y. Li, D. L. Shi, *Small* **2012**, *8*, 760–769; c) Y. Q. Wen, L. P. Xu, C. B. Li, H. W. Du, L. F. Chen, B. Su, Z. L. Zhang, X. J. Zhang, Y. L. Song, *Chem. Commun.* **2012**, *48*, 8410–8412; d) Q. P. Duan, Y. Cao, Y. Li, X. Y. Hu, T. X. Xiao, C. Lin, Y. Pan, L. Y. Wang, *J. Am. Chem. Soc.* **2013**, *135*, 10542–10549; e) Y. P. Chen, C. T. Chen, Y. Hung, C. M. Chou, T. P. Liu, M. R. Liang, C. T. Chen, C. Y. Mou, *J. Am. Chem. Soc.* **2013**, *135*, 1516–1523; f) L. F. Chen, W. Q. Wang, B. Su, Y. Q. Wen, C. B. Li, Y. B. Zhou, M. Z. Li, X. D. Shi, H. W. Du, Y. L. Song, L. Jiang, *ACS Nano* **2014**, *8*, 744–751.
- [9] a) C. Wang, Z. X. Li, D. Cao, Y. L. Zhao, J. W. Gaines, O. A. Bozdemir, M. W. Ambrogio, M. Frascioni, Y. Y. Botros, J. I. Zink, J. Fraser Stoddart, *Angew. Chem.* **2012**, *124*, 5556–5561; *Angew. Chem. Int. Ed.* **2012**, *51*, 5460–5465; b) S. H. Hu, S. Y. Chen, X. H. Gao, *ACS Nano* **2012**, *6*, 2558–2565; c) S. H. Hu, B. J. Liao, C. S. Chiang, P. J. Chen, I. W. Chen, S. Y. Chen, *Adv. Mater.* **2012**, *24*, 3627–3632; d) M. Frascioni, Z. C. Liu, J. Y. Lei, Y. L. Wu, E. Strelakova, D. Malin, M. W. Ambrogio, X. Q. Chen, Y. Y. Botros, V. L. Cryns, J. P. Sauvage, J. Fraser Stoddart, *J. Am. Chem. Soc.* **2013**, *135*, 11603–11613; e) C. Chen, L. Zhou, J. Geng, J. S. Ren, X. G. Qu, *Small* **2013**, *9*, 2793–2800; f) L. Ma, M. Kohli, A. Smith, *ACS Nano* **2013**, *7*, 9518–9525.
- [10] a) L. F. Chen, Y. Q. Wen, B. Su, J. C. Di, Y. L. Song, L. Jiang, *J. Mater. Chem.* **2011**, *21*, 13811–13816; b) R. Veneziano, G. Derrien, S. Tan, A. Brisson, J. Devoisselle, J. Chopineau, C. Charnay, *Small* **2012**, *8*, 3674–3682.
- [11] a) D. P. Ferris, Y. L. Zhao, N. M. Khashab, H. A. Khatib, J. F. Stoddart, J. I. Zink, *J. Am. Chem. Soc.* **2009**, *131*, 1686–1688; b) L. Du, S. J. Liao, H. A. Khatib, J. F. Stoddart, J. I. Zink, *J. Am. Chem. Soc.* **2009**, *131*, 15136–15142.
- [12] N. J. Dunn, W. H. Humphries IV, A. R. Offenbacher, T. L. King, J. A. Gray, *J. Phys. Chem. A* **2009**, *113*, 13144–13151.
- [13] a) A. C. Buzaid, *Cancer Control* **2000**, *7*, 185–197; b) C. Susini, L. Buscail, *Ann. Oncol.* **2006**, *17*, 1733–1742; c) D. Lane, *Nat. Biotechnol.* **2006**, *24*, 163–164; d) K. Oberg, *Nat. Rev. Endocrinol.* **2010**, *6*, 188–189; e) M. S. Glickman, C. L. Sawyers, *Cell* **2012**, *148*, 1089–1098.

Received: February 24, 2014

Published online on May 23, 2014